PII: S0032-3861(97)00514-4

Polymer Vol. 39 No. 11, pp. 2149–2153, 1998

0032-3861/98/$19.00+0.00

Elongational flow and birefringence of low density polyethylene and its blends with ultrahigh molecular weight polyethylene†

Masami Okamoto, Akira Kojima and Tadao Kotaka*
Advanced Polymeric Materials Engineering, Graduate School of Engineering, Toyota Technological Institute, Hisakata 2-12-1, Tempaku, Nagoya 468, Japan
(Received 12 March 1997; revised 7 May 1997; accepted 19 June 1997)

Via elongational flow opto-rheometry (EFOR), simultaneous measurements of tensile stress $\sigma(t)$ and birefringence $\Delta n(t)$ were conducted on a low density polyethylene (LDPE) melt and its blends with an ultra-high molecular weight polyethylene (UHMWPE) at 140°C under transient elongational flow with constant tensile strain rate $\dot{\varepsilon}_0$. The transient elongational viscosity $\eta_E(t) = \sigma(t)/\dot{\varepsilon}_0$ of LDPE melt first gradually increases with time t following the linear viscoelasticity rule in that $\eta_E(t)$ is 3 times the shear viscosity development, $3\eta(t)$, at low shear rate $\dot{\gamma}$ up to a certain critical strain, beyond which $\eta_E(t)$ tended to increase rapidly with t. The behaviour was often referred to as strain-induced hardening. For LDPE melt both $\sigma(t)$ and $\Delta n(t)$ *versus* tensile strain $\varepsilon(t)$ $(= \dot{\varepsilon}_0 t)$ curves were dependent on $\dot{\varepsilon}_0$ in such a manner that the stress optical coefficient $C(t)$ $(\equiv \Delta n(t)/\sigma(t))$ was independent either of $\dot{\varepsilon}_0$, $\varepsilon(t)$ or $\sigma(t)$. Addition of UHMWPE up to 10 wt% to LDPE melt increased the levels of both $\sigma(t)$ and $\Delta n(t)$, but the tendency of strain-induced hardening was reduced. The $C(t)$ was again independent either of $\dot{\varepsilon}_0$, $\varepsilon(t)$ or $\sigma(t)$ and also essentially independent of molecular weight (MW) and its distribution (MWD) or the blend ratio. For both LDPE and the blends the $C(t)$ value roughly agreed with that $(= 2.2 \times 10^{-9}\ \mathrm{Pa}^{-1})$ reported for shear flow experiments, thus confirming the validity of the so far established stress optical rule.

(Keywords: elongation; polyethylene; stress optical rule)

INTRODUCTION

A number of studies has been reported on elongational flow behaviour of polymer melts and blends[1–10]. Since polymer melt elongation is one of the most important deformations in polymer processing, the main objective was directed to the understanding of the material behaviour to achieve optimisation of the processing conditions. Because the elongational viscosity is sensitive to the structural details, the studies are also useful for rheological characterisation of polymer melts. In fact, almost 20 years ago, a world-wide attempt was made to understand the structure–processibility relations of molten polymers. To this end, an IUPAC Working Party[1,2] was organised and distributed three model polyethylene (PE) samples which appeared similar in structure but exhibited quite different processibility. In the survey of using varieties of methodologies available at that time, only Meissner's elongational flow rheometry could resolve their difference[1,2]. In addition, elongational flow rheometry is also useful for evaluation of various molecular theories[11,12] and constitutive models[13–16] of polymer melt rheology.

Usually transient elongational viscosity of a polymer melt first gradually increases with time following the linear viscoelasticity rule between shear and tensile viscosities up to a certain critical strain, beyond which the viscosity tends to increase rapidly with time. The rapid increase was often referred to as strain induced hardening.

On the other hand, rheo-optical methods, especially birefringence[17–19], has become a standard technique in the study of polymer rheology to supplement the mechanical methods. Birefringence, employed as one of the techniques in rheometry, relies on the validity of the stress optical rule which predicts proportionality between the anisotropic refractive index and stress tensors of flowing polymeric liquids[12,17,18]. The proportionality constant, called stress optical coefficient C, has been determined on varieties of polymer melts and solutions in steady as well as in transient shear flows[17–21]. The coefficient C was found to be independent either of time or shear rate even within the regime of highly non-Newtonian or nonlinear viscoelasticity[12,17–21].

However, critical tests of the stress optical rule were rather sparse for elongational flows and conflicting conclusions were found in the literatures[22–25]. In some reports[22,23], we find *nonlinear* stress optical coefficient that often decreased with increasing strain rate, while in some others[24,25] we find a *constant* stress optical coefficient independent either of time, strain rate or stress but weakly dependent on temperature as requested by the stress optical rule[12]. For example, Koyama and Ishizuka[25] carried out a pioneering work on simultaneous measurements of transient tensile stress and birefringence on a low density polyethylene (LDPE) melt under elongational flow at constant strain rate between 120 and 150°C, and reported C of $1.3 \times 10^{-9}\ \mathrm{Pa}^{-1}$ independent of strain rate within 0.002 to 0.2 s^{-1} and only weakly dependent on temperature[25]. Very recently, Kroeger *et al.*[26] discussed stress optical behaviour of polystyrene (PS) melts under uniaxial elongational flow and reported nonlinear stress optical coefficient.

Recently we also developed a new technique of 'elongational flow opto-rheometry' which enabled us to

* To whom correspondence should be addressed
† Elongation Flow Opto-Rheometry for Polymeric Liquids, Part 3

make simultaneous measurements of transient tensile stress and birefringence as a function of time under elongational flow at constant tensile strain rate[27]. The new rheometer, which we called elongational flow opto-rheometer (EFOR), was a combination of a Meissner's new elongational rheometer of gas cushion type[28] commercialised as RME from Rheometric Scientific and a high precision birefringence apparatus of a reflection-double beam path type installed in RME by mounting a small reflecting mirror at the centre of its sample supporting table. In our preliminary experiments[27] we applied EFOR to analyse elongation behaviour of PS and LDPE melts and poly(ethylene terephthalate) (PET) in supercooled state.

In this paper we describe our renewed attempts of testing via EFOR the stress optical rule for transient elongational flow of LDPE melts which has long chain branchings and broad molecular-weight distribution. We also examined the behaviour of its blends with an ultra-high molecular weight PE to clarify the features of strain-induced hardening and segment orientation behaviour in these polyethylene melts.

EXPERIMENTAL

Materials

Samples used were a commercial grade low density polyethylene (LDPE; melt flow index MFI = 0.4 g/10 min, bulk density at 25°C $\rho_{25°C}$ = 0.919 dl g^{-1} and melting temperature T_m = 109.3°C) supplied by Asahi Chemical Co. and a ultrahigh-molecular-weight PE (UHMWPE) (weight-average molecular weight M_w = 2000 K, T_m = 144°C) supplied by Mitsui Petrochemical Co. to prepare blends with LDPE.

In sample preparation for EFOR, pellets were preheated to 150°C for 3 min and hot-pressed at 5 MPa for 3 min to make a sheet of 1.0–0.8 mm thickness. Then the sheet was cut into strips of 60 mm × 7.0 mm size. To prepare blend samples, a prescribed amount of the two polymers was dissolved in decalin at 120°C and stirred for 1 h to make a homogeneous solution of approximately 1–1.7 wt% total concentration. The total concentration was adjusted, depending on the blend ratio, in such a way that the reduced concentration c/c^* of UHMWPE in the blend (with c^* being its coil overlapping concentration) was well below unity so that the solution was sufficiently dilute with respect to UHMWPE: c/c^* varied from 0.033 for 99/1 (LDPE/UHMWPE) blend to 0.23 for 90/10 blend. The polymer was precipitated from the solution at ambient temperature in a large excess of ethanol. The precipitate was recovered and dried at 80°C for 1 day under a reduced atmosphere of 10^{-4} Torr. Obtained blends of LDPE/UHMWPE ratio of 99/1 to 90/10 were press-moulded between polyimide films (Kapton®HN, Toray-DuPont) at 150°C for 8 min and then annealed at 100°C for 10 min to release residual stresses. The moulded sheet of thickness 1.0–0.8 mm was cut into thin strips of 60 mm × 7.0 mm size for later EFOR measurements.

EFOR and other rheometry

In each EFOR run a sample strip was set at a desired temperature between 130 and 150°C ($> T_m$ of the blends) and annealed *in situ* for 30 s which was just long enough for melting the strip to obtain a clear transparent specimen before starting the run. The details are described elsewhere[27,29].

Dynamic viscoelastic measurements were carried out on a Rheometrics Dynamic Analyser (RDAII) with a cone-plate geometry of cone angle 0.1 rad and diameter 25.0 mm operated in the temperature range between 130 and 150°C under nitrogen atmosphere. The strain amplitude was less than 20%. The transient shear viscosity $\eta(\dot{\gamma}, t)$ was also determined in the same temperature range with RDAII operated at a shear rate $\dot{\gamma}$ less than 0.01 s^{-1}. Under these conditions all the melts were Newtonian or linear viscoelastic.

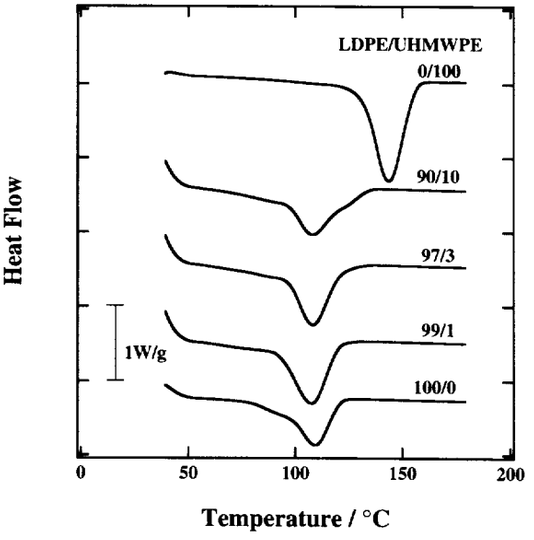

Figure 1 D.s.c. thermograms of LDPE and its blends with UHMWPE (<10 wt%) covering the PE melting region (40~180°C)

TMDSC analysis

Molten LDPE/UHMWPE blends of small UHMWPE content (< 10 wt%) were all transparent and two-phase morphology was not observed under an optical microscope. The blends seemed to be mixed well on the microscopic level. To obtain further information on the melting behaviour of these blends, we slowly cooled transparent molten blends and annealed for a sufficiently long time at 80°C to ensure the samples were fully crystallised and then subjected them to thermal analysis on a temperature-modulated differential scanning calorimeter (TMDSC) (MDSC™; TA 2920, TA Instruments)[30]. The details are described elsewhere[29].

Examples of thermograms covering the PE melting region are shown in *Figure 1*. All blends except the 90/10 blend exhibit a single melting peak with the peak temperature slightly below that of LDPE (T_m = 109.3°C). The melting peak of the 90/10 blend accompanies a small shoulder in the region below T_m of UHMWPE (144°C). These results reflect the melting point depression in miscible blends of two crystalline polymers with different crystallisation habit[31]. As judged from the melting behaviour, the blends with 99/1 to 90/10 are all homogeneous, at least in the range of temperature above T_m of LDPE examined here.

RESULTS

The EFOR behaviour of LDPE melt elongation

Figure 2 shows double-logarithmic plots of transient elongational viscosity $\eta_E(t)$ ($= \sigma(t)/\dot{\varepsilon}_0$) and birefringence $\Delta n(t)$ observed at 140°C with different Hencky strain rates $\dot{\varepsilon}_0$ ranging from 0.005 to 1.0 s^{-1}. The solid line in the figure is the three-fold linear-viscoelastic shear viscosity $3\eta(t)$ with a constant shear rate $\dot{\gamma}$ = 0.01 s^{-1} and the three-fold

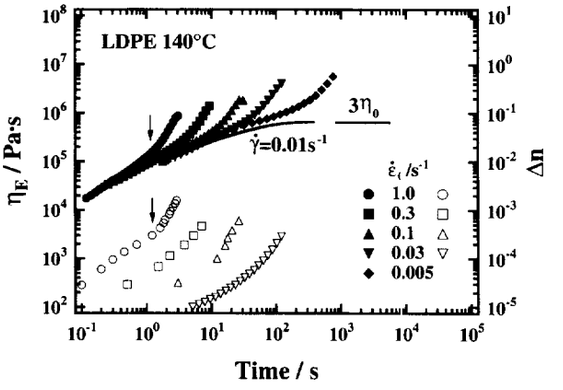

Figure 2 Double logarithmic plots of transient elongational viscosity $\eta_E(t)$ $(=\sigma(t)/\dot{\varepsilon})$ (solid symbols) and birefringence $\Delta n(t)$ (open symbols) against time t for LDPE elongated at 140°C with various Hencky strain rates $\dot{\varepsilon}_0$ as indicated. The solid line indicates 3 times the shear viscosity, $3\eta_0(t)$, determined at the shear rate $\dot{\gamma} = 0.01\ s^{-1}$ at 140°C. The arrows indicate the deformation times at which $\eta_E(t)$ and $\Delta n(t)$ data at $\dot{\varepsilon} = 1.0\ s^{-1}$ begin to deviate from the linear relation (see text)

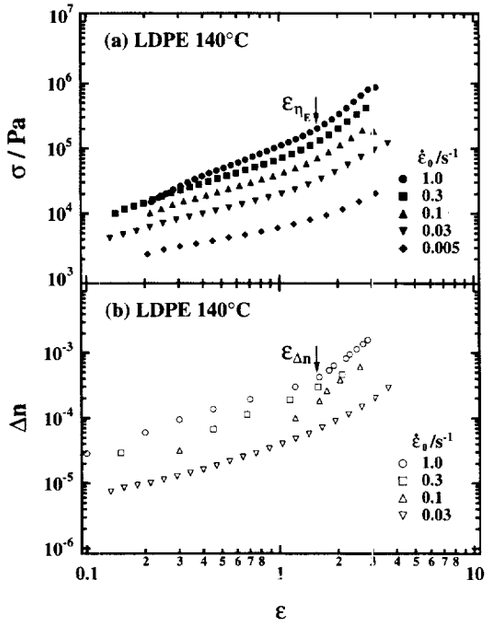

Figure 3 Double logarithmic plots of (a) $\sigma(t)$ and (b) $\Delta n(t)$ against Hencky strain $\varepsilon(t) = \dot{\varepsilon}_0 \cdot t$ replotted from the same LDPE data shown in *Figure 2*. Note that at the Hencky strain of $\varepsilon_{\eta E} \approx \varepsilon_{\Delta n} \approx 1.6$, the $\sigma(t)$ and $\Delta n(t)$ data begin to deviate from the linear relation

zero-shear viscosity $3\eta_0$ obtained at 140°C. In the early stage, elongational viscosity $\eta_E(t)$ tends to follow the linear viscoelasticity rule, $\eta_E(t) = 3\eta(t)$, which is Trouton's rule in the limit of steady state $(t \rightarrow \infty)$[32]. However, $\eta_E(t)$ exhibits a tendency of upward deviation or *up-rising* from $3\eta_0(t)$ at a different *up-rising* time $t_{\eta E}$ depending on $\dot{\varepsilon}_0$, as shown with an arrow for the curve with $\dot{\varepsilon}_0 = 1.0\ s^{-1}$. This strong upward deviation in $\eta_E(t)$ was often called 'strain-induced hardening'[33]. On the other hand, $\Delta n(t)$ first increases with t rather slowly but after a certain deformation time $t_{\Delta n}$, they also begin to deviate upwards depending on $\dot{\varepsilon}_0$. Again, the arrow in the figure indicates $t_{\Delta n}$ for the curve with $\dot{\varepsilon}_0 = 1.0\ s^{-1}$. Note that t_{η_E} and t_{Δ_n} are in agreement with each other.

Figure 3 shows double logarithmic plots of tensile stress $\sigma(t)$ (*Figure 3a*) and birefringence $\Delta n(t)$ (*Figure 3b*) against Hencky strain $\varepsilon(t) = \dot{\varepsilon}_0 t$. Neither $\sigma(t)$ nor $\Delta n(t)$ development profiles cannot be reduced with $\varepsilon(t)$ but exhibit strong $\dot{\varepsilon}_0$-dependence. This feature was also the case for polystyrene (PS) melts[27]. In both $\sigma(t)$ and $\Delta n(t)$ *versus* $\varepsilon(t)$ relations we see that up-rising appears to take place at around $\varepsilon_{\eta_E}(=\dot{\varepsilon}_0 \cdot t_{\eta_E}) \cong \varepsilon_{\Delta_n}(=\dot{\varepsilon}_0 \cdot t_{\Delta_n}) \cong 1.6$ in Hencky unit, independent of $\dot{\varepsilon}_0$, as indicated with the arrows in the figure. In polystyrene (PS) melts, the tendency of strain hardening was rather weak compared with LDPE melt, but nevertheless similar behaviour was observed[27].

The EFOR behaviour of LDPE/UHMWPE blends

Figure 4 shows the LDPE/UHMWPE (90/10) blend double logarithmic plots of $\eta_E(t)$ and $\Delta n(t)$ *versus* t obtained

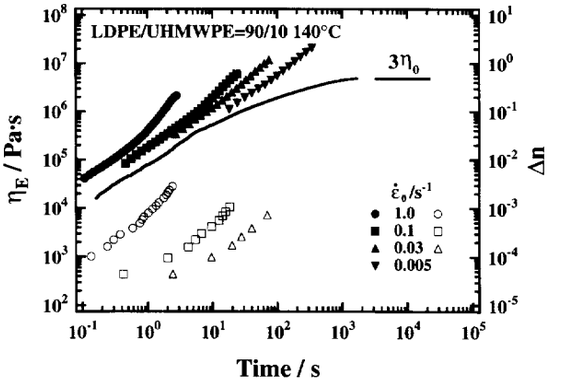

Figure 4 Double logarithmic plots of $\eta_E(t)$ $(=\sigma(t)/\dot{\varepsilon})$ (solid symbols) and $\Delta n(t)$ (open symbols) against time t for LDPE/UHMWPE 90/10 blend elongated at 140°C with various $\dot{\varepsilon}_0$ as indicated. The solid line again indicates $3\eta_0(t)$ determined at $\dot{\gamma} = 0.001\ s^{-1}$ at 140°C. Note that a significant gap is seen between $\eta_E(t)$ and $3\eta_0(t)$

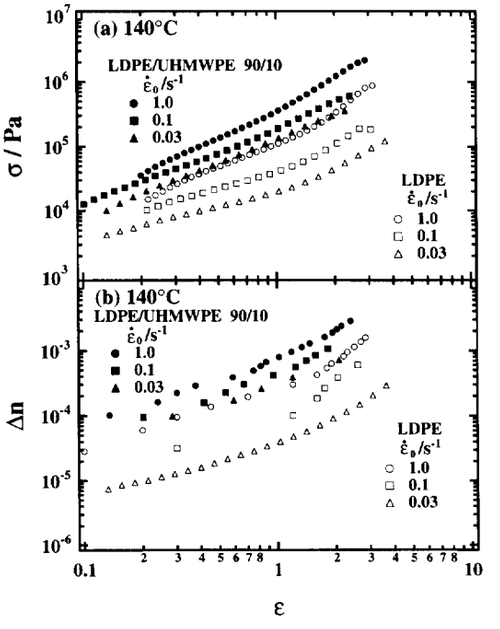

Figure 5 Comparison of the double logarithmic plots of (a) $\sigma(t)$ and (b) $\Delta n(t)$ against $\varepsilon(t) = \dot{\varepsilon}_0 t$ replotted from LDPE shown in *Figure 3* (open symbols) and LDPE/UHMWPE 90/10 blend in *Figure 4* (solid symbols)

at 140°C with different $\dot{\varepsilon}_0$ ranging from 0.005 to 1.0 s^{-1}. In the figure, we also show the three-fold linear viscoelastic shear viscosity $3\eta(t)$ obtained at 140°C with a constant shear rate $\dot{\gamma}$ of 0.001 s^{-1}. Unlike in LDPE shown in *Figure 2*, a small but significant discrepancy is seen in *Figure 4* between the early stages of $\eta_E(t)$ and $3\eta(t)$ profiles. Although the results are not shown here, the discrepancy was found even in LDPE/UHMWPE (99/1) blend. In the early stages, both $\eta_E(t)$ and $3\eta_0(t)$ run parallel with t and $\eta_E(t)$, $3\eta_0(t) \propto t^{\nu}$ with $\nu \cong 0.79$ for 99/1 blend and $\nu \cong 0.68$ for 90/10 blend. In the early stage of 90/10 blend, $\eta_E(t)$ is larger than $3\eta_0(t)$ by a factor of 3–4. For 99/1 blend, the difference was smaller.

For these blends, $\eta_E(t)$ also exhibits a tendency of upward deviation or *up-rising*, again, at a different *up-rising* time $t_{\eta E}$ dependent on $\dot{\varepsilon}_0$. However, the tendency is rather obscured compared with the LDPE melt (*cf. Figures 2, and 4*). In the early stages before $t_{\eta E}$, $\eta_E(t)$ increases more rapidly with t as UHMWPE content of the blend is increased, while in the later stages after $t_{\eta E}$ the tendency of strong up-rising or strain hardening is rather suppressed and $\eta_E(t)$ increases more slowly with increasing UHMWPE content.

Figure 5a shows tensile stress $\sigma(t)$ and *Figure 5b* birefringence $\Delta n(t)$ against Hencky strain $\varepsilon(t) = \dot{\varepsilon}_0 t$ plotted in a double logarithmic form for 90/10 blend at 140°C (closed symbols). For comparison LDPE data in *Figure 3* are replotted (open symbols) in the same figure. Addition of UHMWPE increases $\sigma(t)$ and $\Delta n(t)$ to some extent, but their dependence on $\dot{\varepsilon}_0$ becomes somewhat weaker and also their dependence on $\varepsilon(t)$ especially after the critical Hencky strain $\varepsilon_{\eta E}(=\dot{\varepsilon}_0 t_{\eta E})$ for $\eta_E(t)$ has become much weaker with increasing UHMWPE content compared with LDPE melt. In *Figure 6a*, $\sigma(t)$ data and in *Figure 6b* $\Delta n(t)$ data obtained at 140°C with $\dot{\varepsilon}_0 = 1.0\ s^{-1}$ for LDPE and other three blends of the blend ratio up to 90/10 are replotted against $\varepsilon(t)$ in a double logarithmic form. Again $\sigma(t)$ and $\Delta n(t)$ *versus* $\varepsilon(t)$ curves are still dependent on $\dot{\varepsilon}_0$ and on $\varepsilon(t)$ especially after the critical Hencky strain $\varepsilon_{\eta E}(=\dot{\varepsilon}_0 t_{\eta E})$ with increasing UHMWPE content. As seen in *Figures 5 and 6*, addition of a small amount of UHMWPE also increases $\Delta n(t)$. The dependence of $\Delta n(t)$ on $\varepsilon(t)$ in the later stage after the up-rising Hencky strain $\varepsilon_{\Delta n}$ becomes less clear with increasing UHMWPE content. The value of $\varepsilon_{\eta E}$ itself varies from ~1.6 for LDPE to ~1.1 for 90/10 blend, and correspondingly the value of $\varepsilon_{\Delta n}$ for $\Delta n(t)$ also varies from ~1.6 for LDPE to ~1.1 for 90/10 blend, although the tendency is less clear.

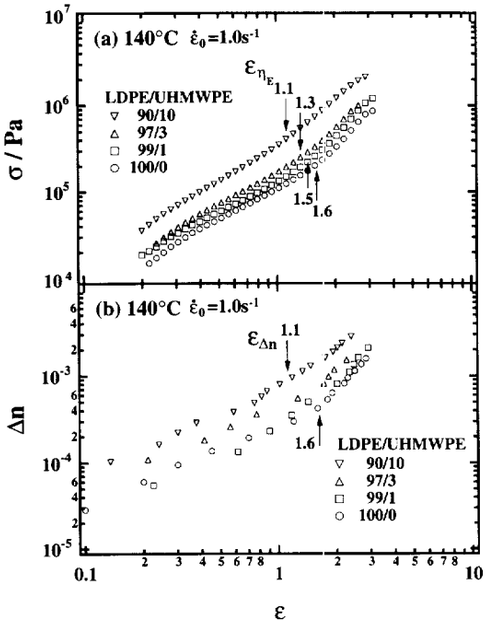

Figure 6 Comparison of (a) $\sigma(t)$ and (b) $\Delta n(t)$ against $\varepsilon(t) = \dot{\varepsilon}_0 t$ data collected at $\dot{\varepsilon}_0 = 1.0\ s^{-1}$ for LDPE and its blends with UHMWPE of the blend ratios (<10 wt%) as indicated. The arrows in panel (a) and (b) indicate the critical Hencky strain $\varepsilon_{\eta E}$ for elongational viscosity and $\varepsilon_{\Delta n}$ for birefringence, respectively

DISCUSSION

Effect of the blending of UHMWPE and LDPE

As evident from *Figures 4–6*, addition of a small amount of UHMWPE increases both $\sigma(t)$ and $\Delta n(t)$, but reduces the tendency of upward deviation or *up-rising* especially after $\varepsilon_{\eta E}$ or $\varepsilon_{\Delta E}$ and also the dependence of $\sigma(t)$ and $\Delta n(t)$ on $\varepsilon(t)$. However, the tendencies are obscured as compared to LDPE melt (*cf. Figures 2, and 4*). The $\eta_E(t)$ appears to be three times higher than $\eta(t)$. The value of $\eta_{\eta E}$ or $\varepsilon_{\Delta n}$ became somewhat smaller with increasing UHMWPE content. These results are quite interesting in light of our attempts to understand the nature of strain induced hardening in polymer melt elongation. In PS melt elongation we hardly see strain induced hardening, which, however, becomes prevailing, especially in the polymers with long chain branchings such as LDPE. The strain induced hardening behaviour was interpreted by Larson[33,34] as the consequence of the hindrance effect in entangled branched chains, which may retard their conformational relaxation by inhibiting repetition. This feature of reducing strain induced hardening appears to be common for melt elongation of linear-chain polymers[27], in which any structural anomaly such as flow-induced crystallisation does not take place as opposed to the case of supercooled poly(ethylene terephthalate)[28].

Stress optical rule

According to the network theory of rubber-like elasticity[35], both $\Delta n(\varepsilon)$ and $\sigma(\varepsilon)$ in large deformation are proportional to the square of the stretch ratio $\lambda(=\exp[\varepsilon])$, which immediately leads for the present polymer melt elongation to the stress optical coefficient $C(t)$ $(=\Delta n(\varepsilon)/\sigma(\varepsilon))$ being a constant, independent of either $\dot{\varepsilon}_0$ or $\varepsilon(t)$. In polymer melt rheology, it has been believed that the stress optical rule holds not only for rubbers[35] but also more general problems of polymeric liquid rheology[12]. According to the currently established stress optical rule[12], the stress optical coefficient $C(t)$ is independent either of time or of the magnitude of strain and strain rate, and is a function of the local condition and the temperature, and thus independent of the global features of the molecular structure such as molecular weight (MW), and its distribution (MWD), long chain branching and degree of crosslinking.

Figure 7 shows double logarithmic plots of $C(t)$ $(=\Delta n(t)/\sigma(t))$ *versus* $\sigma(t)$ obtained at 140°C for LDPE (*Figure 7a*) and its blends with UHMWPE of ratio 90/10 (*Figure 7b*). Also compare our data with the reported value of $C(=\Delta n_{13}/[\sigma_{11}-\sigma_{33}] = 2.2 \times 10^{-9}\ Pa^{-1})$ for PE melts determined for shear flow[18] indicated with an arrow in each panel of the figures. We clearly see that our $C(t)$ values are independent of both $\dot{\varepsilon}_0$ and $\sigma(t)$ and also independent of MW, MWD and/or the blend ratio, on either of which $C(t)$ should not depend according to the stress optical rule[12]. The present results

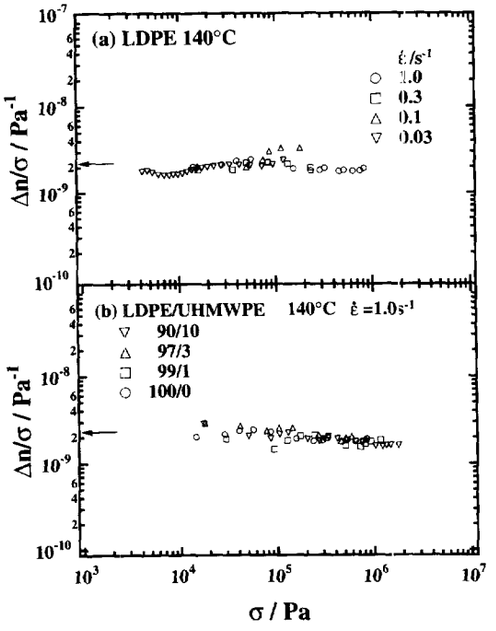

Figure 7 The stress optical coefficient $C(t) \equiv \Delta n(t)/\sigma(t)$ for (a) LDPE, and (b) LDPE/UHMWPE 90/10 blend obtained at 140°C. The arrow in each panel indicates $C = 2.2 \times 10^{-9}$ Pa^{-1} reported for shear flow experiments[18]

show that in spite of the fact that LDPE melt and its blends with UHMWPE exhibit significant tendency of strain-induced hardening, the stress optical rule is still obeyed and the level of $C(t)$ *versus* $\sigma(t)$ conforms with the value reported for shear flow experiments[18] for all the samples examined within the range of strain rates, Hencky strains and stresses examined here.

CONCLUSIONS

As to the molecular rheological background, the stress optical rule as stated by Doi[12] sets two reservations: namely, for the rule being valid, (a) the relation between the orientation of the bond vectors and that of the end-to-end vector of the Rouse segments is linear and (b) the form birefringence is neglected[12]. In addition, Doi also pointed out that although the excluded volume interactions do not violate the validity of the stress optical rule but they do affect the values of C, which is, for example, sensitive to the nematic-like interaction causing the neighbouring chains to orient in the direction of elongation[12]. Under high strain rate elongation of high MW and/or well-entangled polymer melts, these conditions are not always met[18].

The most significant difference between the previous and present studies is that we employed elongational flow with extremely high strain rates up to a stretch ratio λ of 200 or total strain of 5 in Hencky unit, for which the assumption (a) might be violated. In broad MWD samples nematic-like interaction may enhance the orientation and thus increase $\Delta n(t)$ even in the region of small ε. On the other hand, presence of the branchings and/or incorporation of high MW components into LDPE melt under high rate elongation might suppress tensile stress relaxation to occur, and thus might increase $\sigma(t)$. In our experiments these two effects just cancel each other and thus the value of $C(t)$ is independent of $\sigma(t)$, in agreement with the value of C expected from previous small shear deformation experiments.

ACKNOWLEDGEMENTS

The EFOR was constructed with the financial support of the Ministry of Education, which the authors acknowledge with thanks.

REFERENCES

1. Meissner, J., *Rheologica Acta*, 1969, **8**, 78.
2. Meissner, J., *Pure and Applied Chemistry*, 1975, **43**, 553.
3. Evarage, A. E. and Ballman, R. L., *Applied Polymer Science*, 1976, **20**, 1137.
4. Ide, Y. and White, J. L., *Applied Polymer Science*, 1978, **22**, 1061.
5. Laun, H. M. and Muenstedt, H., *Rheologica Acta*, 1978, **17**, 415.
6. Ishizuka, O. and Koyama, K., *Polymer*, 1980, **21**, 164.
7. Pearson, G. H. and Connelly, R. W., *Journal of Applied Polymer Science*, 1982, **27**, 969.
8. Kanai, T. and White, J. L., *Polymer Engineering Science*, 1984, **24**, 1185.
9. Utracki, L. A., Dumoulin, M. M. and Toma, P., *Polymer Engineering Science*, 1986, **26**, 34.
10. Utracki, L. A. and Schlund, B., *Polymer Engineering Science*, 1987, **27**, 1512.
11. Rouse, P. E. Jr., *Journal of Chemical Physics*, 1953, **21**, 1272.
12. Doi, M. and Edwards, S. F., *The Theory of Polymer Dynamics*. Clarendon Press, Oxford, 1986.
13. Lodge, A. S., *Elastic Liquids*. Academic Press, London, 1964.
14. Bernstein, B., Keasley, E. A. and Zapas, L. J., *Transactions of the Society of Rheology*, 1965, **7**, 391.
15. Bogue, D. C. and White, J. L., *Engineering Analysis of Non-Newtonian Fluids*, Argadograph Series 144, NATO, 1970.
16. Larson, R. G., *Constitutive Equations for Polymer Melts and Solution*. Butterworth, Stonenham, MA, 1988.
17. Wales, J. L. S., *The Application of Flow Birefringence to Rheological Studies of Polymer Melts*. Delft University, Rotterdam, 1976.
18. Janeschitz-Kriegel, H., *Polymer Melt Rheology and Flow Birefringence*. Springer, New York, 1983.
19. Zebrowski, B. E. and Fuller, G. G., *Journal of Polymer Science, Polymer Physics Edition*, 1981, **19**, 531.
20. Chow, A. W. and Fuller, G. G., *Journal of Rheology*, 1984, **28**, 23.
21. Frattini, P. L. and Fuller, G. G., *Journal of Rheology*, 1984, **28**, 61.
22. Katayama, K., Amano, T. and Nakamura, K., *Applied Polymer Symposia*, 1973, **20**, 237.
23. Matsumoto, T. and Bogue, D. C., *Journal of Polymer Science, Polymer Physics Edition*, 1977, **15**, 1663.
24. Ishizuka, O. and Koyama, K., *Seni-i-Gakkaishi*, 1976, **32**, T-49.
25. Koyama, K. and Ishizuka, O., *Journal of Polymer Science, Part B, Polymer Physics*, 1989, **27**, 297.
26. Kreger, M., Lupa, C. and Muller, R., *Macromolecules*, 1997, **30**, 526.
27. Kotaka, T., Kojima, A. and Okamoto, M., *Rheologica Acta*, 1997, in press.
28. Meissner, J., *Rheologica Acta*, 1994, **33**, 1.
29. Okamoto, M., Kubo, H. and Kotaka, T., *Polymer*, 1997, in press.
30. Wunderlich, B., Jin, Y. and Boller, A., *Thermochimica Acta*, 1994, **238**, 277.
31. Nishi, T., *Journal of Macromolecular Science, Physics Edition*, 1980, **B17**, 517.
32. Trouton, F. T., *Proceedings of the Royal Society*, 1906, **A77**, 426.
33. Larson, R. G., *Journal of Rheology*, 1984, **28**, 545.
34. Khan, S. A., Prud'homme, R. K. and Larson, R. G., *Rheologica Acta*, 1987, **26**, 144.
35. Treloar, L. R. G., *The Physics of Rubber Elasticity*, 2nd edn. Claredon Press, Oxford, 1958, p. 197.